International Journal of Pharmaceutics 402 (2010) 205–212

Contents lists available at ScienceDirect

International Journal of Pharmaceutics

journal homepage: www.elsevier.com/locate/ijpharm

Pharmaceutical Nanotechnology

Penetration and distribution of PLGA nanoparticles in the human skin treated with microneedles

Wei Zhang[a,1], Jing Gao[b,1], Quangang Zhu[a], Min Zhang[a], Xueying Ding[b], Xiaoyu Wang[a], Xuemei Hou[a], Wei Fan[a], Baoyue Ding[a], Xin Wu[a], Xiying Wang[a], Shen Gao[a,*]

[a] Department of Pharmaceutics, Changhai Hospital, Second Military Medical University, Shanghai 200433, PR China
[b] Department of Pharmaceutics, School of Pharmacy, Second Military Medical University, Shanghai 200433, PR China

ARTICLE INFO

Article history:
Received 26 July 2010
Received in revised form
16 September 2010
Accepted 27 September 2010
Available online 12 October 2010

Keywords:
Skin
Microneedles
PLGA
Nanoparticles
Topical drug delivery

ABSTRACT

This study was designed to investigate the penetration and the distribution of poly(D,L-lactic-co-glycolic acid) (PLGA) nanoparticles in the human skin treated with microneedles. Fluorescent nanoparticles were prepared to indicate the transdermal transport process of the nanoparticles. Permeation study was performed on Franz-type diffusion cells *in vitro*. The distribution of nanoparticles was visualized by confocal laser scanning microscopy (CLSM) and quantified by high performance liquid chromatography (HPLC). CLSM images showed that nanoparticles were delivered into the microconduits created by microneedles and permeated into the epidermis and the dermis. The quantitative determination showed that (i) the permeation of nanoparticles into the skin was enhanced by microneedles, but no nanoparticle reached the receptor solution; (ii) much more nanoparticles deposited in the epidermis than those in the dermis; (iii) the permeation was in a particle size-dependent manner; and (iv) the permeation increased with the nanoparticle concentration increasing until a limit value was reached. These results suggested that microneedles could enhance the intradermal delivery of PLGA nanoparticles. The biodegradable nanoparticles would sustain drug release in the skin and supply the skin with drug over a prolonged period. This strategy would prove to be useful for topical drug administration.

1. Introduction

The stratum corneum (SC) barrier plays a critical role in transdermal drug delivery. Many strategies have been used to improve transdermal drug delivery including chemical penetration enhancers and different physical enhancement vehicles such as microneedles (Prausnitz, 2004; Verbaan et al., 2007) and iontophoresis (Kanikkannan, 2002). Drug permeation by these strategies was enhanced, but the drug that had permeated into the skin was gradually absorbed into the systemic circulation and only little could stay in the skin layers. However, the dermatological diseases needed that drug accumulated in the skin to play a local treatment. For example, the pigmentation needed drug accumulate in the skin to inhibit melanin formation. Therefore, it was necessary to develop a strategy to improve the skin retention of the drug.

Nanoparticles have been extensively studied for oral and parenteral administration owing to their sustained drug release (de Jalon et al., 2001; Jenning et al., 2000). This property of nanoparticles could also be utilized for topical drug administration to support the skin with drug over a prolonged period and to maintain a desired drug concentration in the skin. Many researchers had attempted to use nanoparticles for topical drug delivery, and they found that the drug permeation was enhanced by gradual drug release from the nanoparticles on the skin surface, but did not find the nanoparticle carriers inside the skin (Alvarez-Roman et al., 2004b,c; Luengo et al., 2006). This suggested us that as a drug delivery vehicle, the nanoparticle could sustain drug release, but if it was applied as a drug reservoir to treat the skin disease, it must be delivered into the skin layers instead of remaining on the skin surface. Some other researchers attempted to verify the penetration of nanoparticles across the skin, but found that only few of nanoparticles were able to permeate into the skin passively through the hair follicles while most nanoparticles were primarily restricted to the uppermost SC layer and unable to penetrate the skin (Lademann et al., 2007; Toll et al., 2004). An effective approach was needed to assist nanoparticles to overcome the SC barrier.

Microneedles have been used widely to increase the skin permeability of drugs (Chabri et al., 2004; Prausnitz, 2004) which was due to that the microneedles can transiently create microconduits that can penetrate through the SC barrier, extend into the viable epidermis and facilitate the drug permeation. To investigate if the microconduits on the epidermis produced by microneedles could be the channels for nanoparticles to penetrate the membrane, the

* Corresponding author. Tel.: +86 21 81873715; fax: +86 21 81873715.
E-mail address: liullk@126.com (S. Gao).
[1] These authors contributed equally to this work.

0378-5173/$ – see front matter © 2010 Elsevier B.V. All rights reserved.
doi:10.1016/j.ijpharm.2010.09.037

researches *in vitro* have been designed and proved that polystyrene nanoparticles could traverse the human epidermal membrane into the receptor compartment (Coulman et al., 2009; McAllister et al., 2003). Then, in the penetration experiments *in vitro* using the full-thickness skin, while the microconduits in the epidermis were produced by ViaDerm™, it was found that polystyrene nanoparticles could diffuse into the dermis as well as into the epidermis (Birchall et al., 2006). All the studies above indicated that microneedles may be an effective vehicle for the intradermal delivery of nanoparticles.

After the skin treated with microneedles, the distribution of nanoparticles in the different skin layers was little reported, even if it had been proved that using microneedles was beneficial to the permeation of nanoparticles (Coulman et al., 2009; McAllister et al., 2003). The amount of the nanoparticles deposited in the skin decided whether the drug accumulated in the skin would reach to the dosage for treatment. This result would decide whether the combination of microneedles with nanoparticles could be an effective approach for topical drug administration.

This study was designed to investigate the penetration and the distribution of nanoparticles in the full-thickness human skin treated with microneedles *in vitro*. The biodegradable and biocompatible poly(D,L-lactic-co-glycolic acid) (PLGA) was used as the nanoparticle carrier. To verify the presence of nanoparticles in the skin, coumarin 6 was selected to be a fluorescent probe to indicate the penetration process of nanoparticles. Observation was done under confocal laser scanning microscopy (CLSM), knowing that little or no sample preparation is needed and there would be little interference with the observation of the nanoparticles. Nanoparticles located in different skin layers were quantified by high performance liquid chromatography (HPLC).

Previous CLSM investigations to examine the polystyrene nanoparticles (diameter 20–200 nm) across the intact porcine skin showed that small particles could be delivered into the hair follicles more favorably than big particles (Alvarez-Roman et al., 2004c), implying that the size of nanoparticles may influence the penetration of nanoparticles through the microconduits. So we used nanoparticles of different sizes to evaluate the effect of the size on the penetration. In addition, various concentrations of nanoparticles were applied in order to achieve the maximal permeation.

2. Materials and methods

2.1. Materials

Materials used in the present study included PLGA (50:50, Mw = 15,000) (DaiGang Biotechnology Co. Ltd., Jinan, China); polyvinyl alcohol (PVA) (1788, Mw = 22,000), 87–89% hydrolyzed (Jingchun Chemical Reagent Co. Ltd., Shanghai, China); and coumarin 6 (Acros Organics Chemical Co. Ltd., New Jersey, USA). All chemicals and solvents were of analytical grade.

2.2. Preparation of coumarin 6-loaded fluorescent PLGA nanoparticles

Coumarin 6-loaded PLGA nanoparticles (NP1) were prepared by a w/o/w emulsification solvent evaporation method as previous described (Blanco, 1997). Briefly, 100 μl aqueous solution was emulsified in 1 ml dichlormethane (DCM) solution containing 100 μg/ml coumarin 6 and 10 mg PLGA by sonication (JYD-900, Zhixin Instrument Co. Ltd., Shanghai, China) for 60 s (300 W) in an ice bath to form the first emulsion (w1/o). The w1/o emulsion was thereafter poured into 4 ml 1% PVA solution (w2) and sonicated for 60 s (200 W) to form a double emulsion (w1/o/w2). The w1/o/w2 double emulsion was then diluted into 40 ml 0.5% PVA solution and stirred for 4 h to evaporate the DCM. Nanoparticles were collected by centrifugation (TGL20M, BAida, China) at 12,000 rpm for 30 min and washed thrice before lyophilization (FD5-3P, SIM, American). 25 mg (NP2) and 40 mg PLGA (NP3) were used to prepare the nanoparticles of different sizes in the same process.

2.3. Characterization of nanoparticles

Freeze-dried nanoparticles were dispersed in deionized water. Average size, zeta potential and polydispersity of nanoparticles were analyzed using a particle size analyzer (Zeta Sizer 3000HS, Malvern, UK). The nanoparticle suspension was stored at room temperature for 48 h and then was measured again. At least three different batches were analyzed to obtain a mean value. Surface morphology was determined by transmission electronic microscopy (TEM) (JEM2010, JEOL, Japan).

2.4. Determination of encapsulation efficiency and drug loading efficiency of coumarin 6

The encapsulation efficiency (EE) and the drug loading efficiency (LE) of coumarin 6 in the nanoparticles were determined by HPLC. The nanoparticles were dissolved in acetonitrile and measured by HPLC in triplicates to determine the content of coumarin 6 (Pang et al., 2008). The HPLC system (SHIMADZU LC-10AT Palo Alto, CA) was equipped with a fluorescence detector and a C18 column (Diamonsil C18, 250 mm × 4.6 mm, 5 μm, Dikma Technologies, CA, USA). The analyses were performed at room temperature, mobile phase water/methanol (5/95, v/v), flow rate 1 ml/min, Ex = 465 nm, Em = 502 nm, Rt 7.1 min. The coumarin 6 peak was quantitatively determined by comparing with a standard curve: $C = 0.0001A + 0.0394$, 0.1–10.0 ng/ml, $r = 0.999$. Six parallel samples were conducted. EE and LE were calculated according to the equations: EE = 100% × amount of the drug in nanoparticles/amount of the feeding drug; LE = 100% × amount of the drug in nanoparticles/amount of the nanoparticles.

2.5. In vitro release of coumarin 6 from nanoparticles

To determine the amount and the rate of coumarin 6 releasing from the nanoparticles, an *in vitro* release study was conducted over a 48-h period. The nanoparticles were dispersed in 50 ml 100 mM PBS at pH 7.4, and then the suspension was filled into tubes, incubated at 37 °C and continuously shaken at 100 rpm. At predetermined intervals, 2 ml suspension was taken out, replaced with fresh PBS, and centrifuged at 15,000 rpm for 30 min. The supernatant was decanted for analysis. The amount of coumarin 6 released into the PBS solution was determined by HPLC methodology as previously described. Six parallel samples at each predetermined interval were prepared, and kept away from light throughout the experimental procedure.

2.6. Fabrication of microneedles

Microneedles were fabricated with single-crystal Si as starting material and using a series of photolithography, thin-film deposition, and reactive ion etching techniques (Henry et al., 1998; Xie et al., 2005). After deposition and patterning of star oxide patterns on a Si substrate, the portion of the Si wafers not covered by these patterns was etched away by a reactive ion etching process to form the needle shafts. The microneedle arrays were visualized using a scanning electron microscope (SEM) (XL30, FHILIPS, Holland). An applicator was designed to fix and give a variant pressure to the microneedle arrays. To assess the ability of microneedles to create microconduits across SC, microneedle arrays were fixed onto the applicator, pierced into the human abdominal skin with 15 N

pressure, and then removed. The epidermis was separated from the skin by the hot-plate separation method (Liang, 2005). The pieced skin and the separated epidermis were spread over methylene blue dye and subsequently visualized under the microscope with the SC upside. The pieced skin was fixed in 10% buffered formalin, embedded in paraffin, sectioned, stained by H&E, and observed under the microscope.

2.7. Transdermal transport study in vitro

2.7.1. Preparation and storage of skin samples

Full-thickness skin samples were obtained from a female patient undergone abdominal plastic surgery with ethical committee approval and informed consent. After excision, the subcutaneous fatty tissue of the abdominal region was removed using a scalpel and washed with normal saline immediately. Then the skin was wrapped in aluminum foil, stored in polyethylene bags at −20 °C and used in two weeks (Aguzzi et al., 2008).

2.7.2. Transdermal delivery of nanoparticles in vitro on Franz-type diffusion cells

The human abdominal skin was treated with microneedles at a pressure about 15 N. Once the needles were inserted into the skin, the applicator was held in the position for 1 min to let the microneedles create microconduits. The treated skin was then mounted on Franz-type diffusion cells with the SC side facing the donor. The diffusion area was 0.50 cm^2. 700 μl Fluorescent nanoparticle suspension (0.8 mg/ml NP2 dispersed in the 100 mM PBS, pH 7.4) was placed in the donor compartment covered with a parafilm to prevent evaporation. Each receptor chamber was filled with 4.5 ml 100 mM PBS at pH 7.4 and kept at 32 ± 0.5 °C by a circulating-water jacket. The stirring of the receptor solution was maintained at 320 rpm. The skin without microneedles treatment was used as the negative control. Six parallel samples were conducted in the experiment.

2.7.3. Skin penetration of nanoparticles

At the 48-h interval, Franz-type cells were dismantled. The SC surface of the skin was thoroughly wiped with PBS and blotted with cotton swabs. The skin samples were placed on a microscope slide, observed under a fluorescence microscope, and then scanned at 488 nm excitation wavelength by CLSM (FluoView™ FV1000, OLYMPUS, Japan) to visualize the distribution of the fluorescent nanoparticles in the skin (Alvarez-Roman et al., 2004a,c). Images were obtained in the *xy*-plane (parallel to the plane of the skin surface). The initially scanned skin surface ($z = 0$ μm) was defined as the imaging plane of the brightest fluorescence with a morphologic characteristic of the SC surface. Subsequently, Scanning was conducted once at the interval of 4.27 μm from the skin surface through the *z*-axis perpendicular to the *xy*-plane.

2.7.4. Distribution of nanoparticles in the receptor solution and in the skin

To quantitatively assess the distribution of the nanoparticles, the amount of nanoparticles in the receptor solution and that in the different skin layers were determined by HPLC.

At predetermined time intervals, Franz-type cells were dismantled. A 500 μl sample was collected from the receptor solution, dissolved in 2.5 ml acetonitrile and then measured by HPLC to determine the content of coumarin 6. The effective area of the skin was cut off and the SC was wiped with deionized water for five times. The epidermis was separated from the dermis using the hot-plate separation method (Liang, 2005). The skin was placed on the hot plate (heated in 50 °C water) for 5 min. Then the epidermis was peeled and scraped off from the skin with tweezers. The epidermis and the remaining dermis were cut into small pieces, homogenized in 2 ml deionized water under ice bath for 10 min, and centrifuged at 15,000 rpm for 20 min. 500 μl clear supernatant was mixed with 2.5 ml acetonitrile for protein precipitation, subsequently subjected to the vortex for 30 s, and centrifuged at 15,000 rpm for 20 min. The clear supernatant thus obtained was analyzed by HPLC as described above to determine the content of coumarin 6. The extraction protocol verified by the adding sample recovery test was able to extract more than 99% of the applied dose.

The amount of nanoparticles was calculated according to the equation: amount of nanoparticles = 100 × content of coumarin 6/LE.

The percentage of the applied nanoparticles delivered into the receptor solution and depositing in the skin was calculated and plotted versus time.

2.7.5. Effect of size and concentration of nanoparticles on the penetration

To assess the effect of the nanoparticle size on the permeation and the distribution, a study using nanoparticles of different sizes (NP1, NP2 and NP3) was performed and the concentrations of nanoparticles were all adjusted to 0.8 mg/ml.

To assess the effect of the nanoparticle concentration on the permeation, the nanoparticle suspension (NP2) of different concentrations (range 0.4–3 mg/ml) were applied in the donor.

2.8. Data analysis

The data were presented as mean ± SD. Statistical significances were determined using two-sample *t* test and analysis of variance (ANOVA) with $P < 0.05$ as a significance level.

3. Results and discussion

3.1. Characterization of nanoparticles

Table 1 indicates the physical characterization of the nanoparticles of different formulations. An increasing trend in the mean particle size was observed when the PLGA concentration increased in the nanoparticle formulations. Zeta potentials were all negative and not in the range of −30 and +30 mV, within which suspensions are considered unstable (Sugrue, 1992). The particle size and the polydispersity almost did not change after the nanoparticle suspension stored for 48 h, suggesting that the nanoparticles did not aggregate during the penetration experiment. The surface morphology of NP1 was evaluated by TEM (Fig. 1). EE was more than 60% and significantly increased with the nanoparticle size increasing.

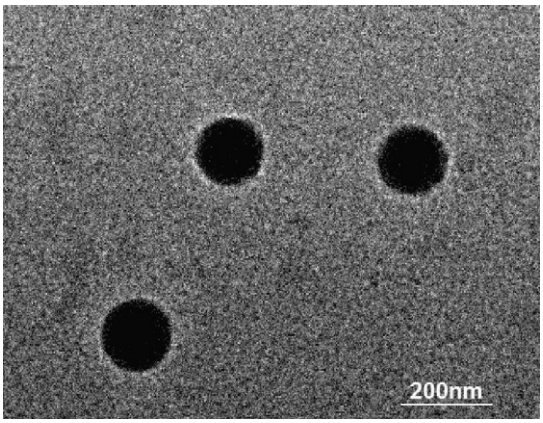

Fig. 1. Image of NP1 by transmission electronic microscopy (TEM).

Table 1
Average size, zeta potential, polydispersity index, EE and LE of different nanoparticle formulations.

Formulation (concentration of PLGA, mg/ml)	Mean size (nm)	Zeta potential (mV)	Polydispersity index	EE (%)	LE (%)
NP1 (10)	160.1 (1.97)	−30.9 (0.85)	0.114 (0.006)	61.40 (0.22)	0.61 (0.00)
NP2 (25)	205.5 (7.47)	−33.3 (0.61)	0.191 (0.007)	81.33 (0.15)	0.33 (0.00)
NP3 (40)	288.2 (6.26)	−36.3 (0.46)	0.225 (0.003)	94.46 (0.30)	0.24 (0.00)

Results are expressed as mean (SD) for three measurements.

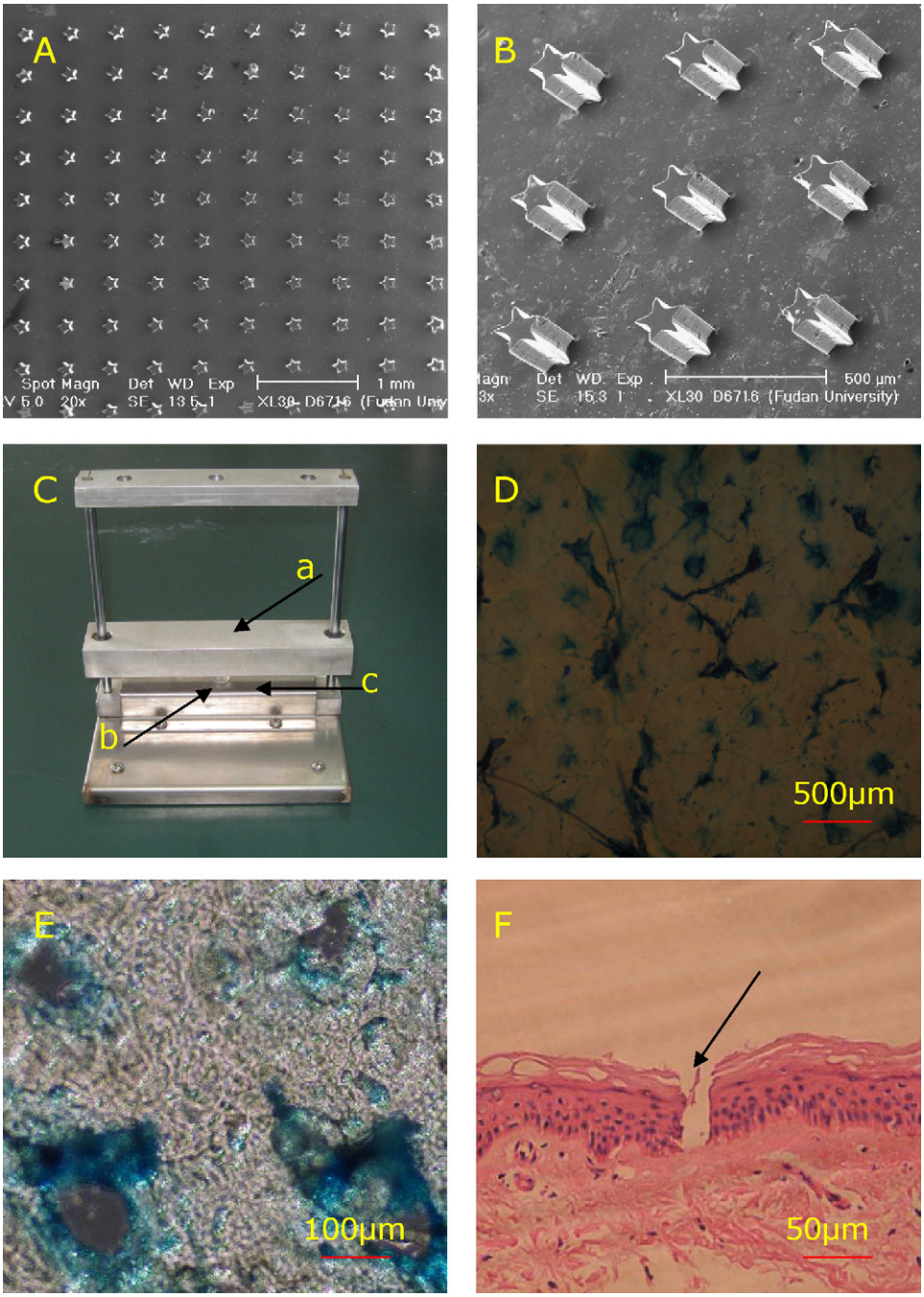

Fig. 2. (A and B) Scanning electron microscope (SEM) images of star silicon microneedles. (C) Photograph of the applicator of the microneedle arrays. The arrow "a" corresponded to the platform on which the weights were placed. The arrow "b" corresponded to the microneedles. The arrow "c" corresponded to the platform on which the skin was placed. (D) Microphotograph of human skin pierced with microneedles and stained by methylene blue (4× objective). (E) Microphotograph of the epidermis separated from the pieced skin (20× objective). (F) Microphotograph of vertical section of the skin pierced with microneedles and stained by H&E (40× objective). The arrow corresponded to microconduit produced by microneedle.

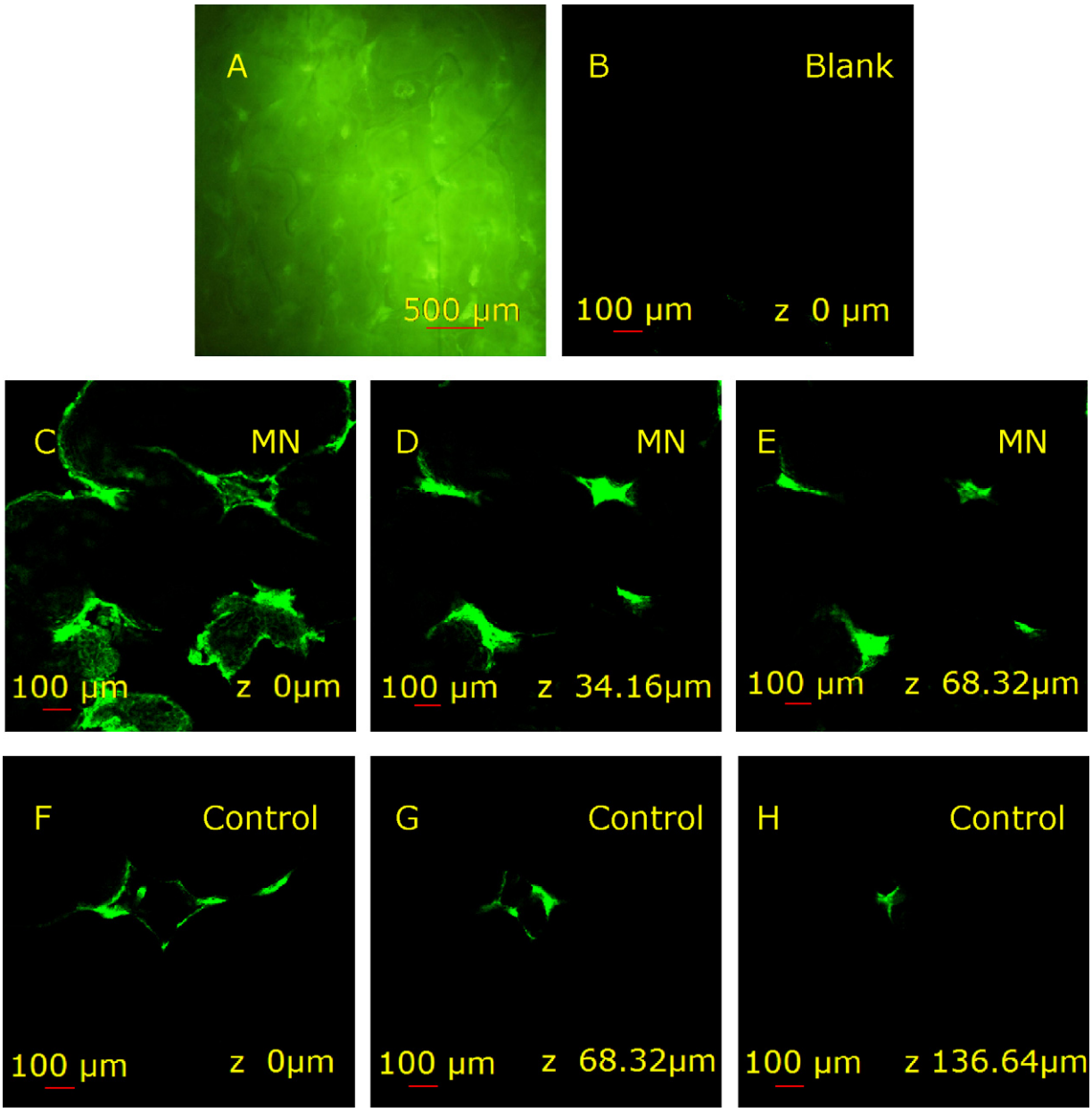

Fig. 3. Images of skin after the coumarin 6 nanoparticles applied for 48 h. (A) Image of the skin in the microneedle group by the fluorescence microscope (4× objective). (B) Image of the blank human abdominal skin scanned at 488 nm excitation wavelength by CLSM. Images of skin at different depth in the microneedle group scanned at 488 nm excitation wavelength by CLSM (10× objective): (C) 0 μm, (D) 34.16 μm and (E) 68.32 μm. Images of skin at different depth in the control group scanned at 488 nm excitation wavelength by CLSM (10× objective): (F) 0 μm, (G) 68.32 μm and (H) 136.64 μm.

3.2. In vitro release of coumarin 6

PBS at pH 7.4 was used to disperse nanoparticles in the subsequent '*Transdermal transport study in vitro*', so we determined the *in vitro* release of coumarin 6 in this solution. It was found that less than 0.5% of the coumarin 6 released from the nanoparticles of the three formulations to the donor solution, which was probably due to that coumarin 6 was lipophilic and hardly dissolved in the water solution. The results would prove that in the subsequent '*Transdermal transport studies in vitro*', the coumarin 6 detected in the skin tissues and in the receptor solution was mainly attributed to the permeation of coumarin 6 nanoparticles rather than the permeation of free coumarin 6 released from the nanoparticles to the donor solution. Therefore, coumarin 6 seems to be a suitable marker for nanoparticles, which is consistent with previous studies (Gao et al., 2006; Panyam et al., 2003).

3.3. Microneedles

The microneedle arrays were characterized, showing that the finished microneedle arrays had a surface area of 25 mm^2 and contained 100 microneedles equally distributing in a 10×10 arrangement, while each needle with a star pattern tip was 200 μm in height (Fig. 2A and B). Fig. 2C shows the photograph of the applicator. The pressure to the microneedles could be changed through changing the weight on the microneedles. Following microneedle treatment at a pressure about 15 N, piercing of the skin was visualized (Fig. 2D–F).

3.4. Penetration of nanoparticles into the skin

Images of the skin under the fluorescence microscope showed that the fluorescence of the nanoparticles was apparent in

locations of microneedle piercing after the application of coumarin 6 nanoparticles for 48 h in the microneedle group (Fig. 3A). Images of the skin at different depths scanned by CLSM showed that the fluorescence of the nanoparticles was inside the microconduits, but no fluorescence was observed in the other areas (Fig. 3C–E), indicating that the SC was the barrier for the transdermal delivery of nanoparticles, and the nanoparticles may be able to be delivered into the skin after the SC broken by microneedles.

The human abdominal epidermis is about 60 μm thick (Fig. 2F). The fluorescence was still observed at the depth of 68.32 μm (Fig. 3E), indicating that nanoparticles not only permeated into the viable epidermis, but also diffused into the dermis.

In the control group, images of the skin at different depths showed that the fluorescence of nanoparticles was not observed in the skin but in the hair follicles (Fig. 3F–H), suggesting that nanoparticles could not penetrate the SC barrier without microneedle treatment, but could passively permeate into the skin by the follicular pathway, which is consistent with the previous investigation (Lademann et al., 2007).

Fluorescence of the skin besides the microconduits was observed under a fluorescence microscope (Fig. 3A), but not observed at 488 nm laser excitation wavelength by CLSM (Fig. 3B), which may be due to that the skin was excited at an extensive range of wavelengths by a fluorescence microscope but only at a single wavelength by CLSM. Thus there was no impact for the survey on the fluorescence from nanoparticles by CLSM.

3.5. Skin penetration

When the human epidermal membrane treated with microneedles was used in the penetration experiment *in vitro*, more than 20% of the applied polystyrene nanoparticles (diameter of between 100 and 150 nm) had been detected in the receptor solution (Coulman et al., 2009). To investigate the ratio of PLGA nanoparticles (diameter in 205.5 nm) in the receptor solution to that in the skin, we used the full-thickness human abdominal skin in the penetration experiment. Although the skin SC barrier had been broken by microneedles and nanoparticles had been delivered into the skin through the microconduits, the results of the penetration showed that no nanoparticle was detected in the receptor solution even if the application period was extended to 48 h. A previous study about the application of PLGA microparticles to the intact skin showed that the microparticles were delivered into the skin, but were not detected in the receptor solution in a period of 24 h (de Jalon et al., 2001). On the basis of these findings, we proposed that the delivery of PLGA nanoparticles through the microconduits created by microneedles is possibly a form of intradermal delivery. The reason may be that the penetration of the nanoparticles was related with the nanoparticle size and the channel size (Coulman et al., 2009; McAllister et al., 2003), so the nanoparticles could penetrate the epidermal membrane through the microconduits created by microneedles and then gradually diffused in the skin layers, but could not penetrate across the dermis in which no microconduits were created and also could not permeate into the receptor solution. Moreover, it is difficult for lipophilic drugs to penetrate the skin tissue (Liang, 2005). PLGA is lipophilic, so nanoparticles may gradually accumulate in the skin layers rather than penetrate into the receptor solution. Taken together these, the penetration of nanoparticles may be influenced by the effect of the microneedle on the skin, the nanoparticle size and the physico-chemical properties of the nanoparticle material.

3.6. Skin deposition

Fig. 4A and B shows that the percentage of the applied nanoparticles depositing in the epidermis and in the dermis in the microneedle groups was significantly higher than that in the control groups ($P < 0.01$) at each interval, suggesting that the skin penetration of nanoparticles could be significantly increased by microneedles. The permeation in the negative control group was supposed to be due to the permeation via the hair follicles as observed by CLSM. The percentage of the applied nanoparticles in the microneedle groups was higher than that in the control groups, which may be due to that microneedles were in the degree of micrometer and could create much higher density channels than the hair follicles. Based on this result, microneedles are seemed to be more effective vehicles than the hair follicles to assist nanoparticles to penetrate into the skin.

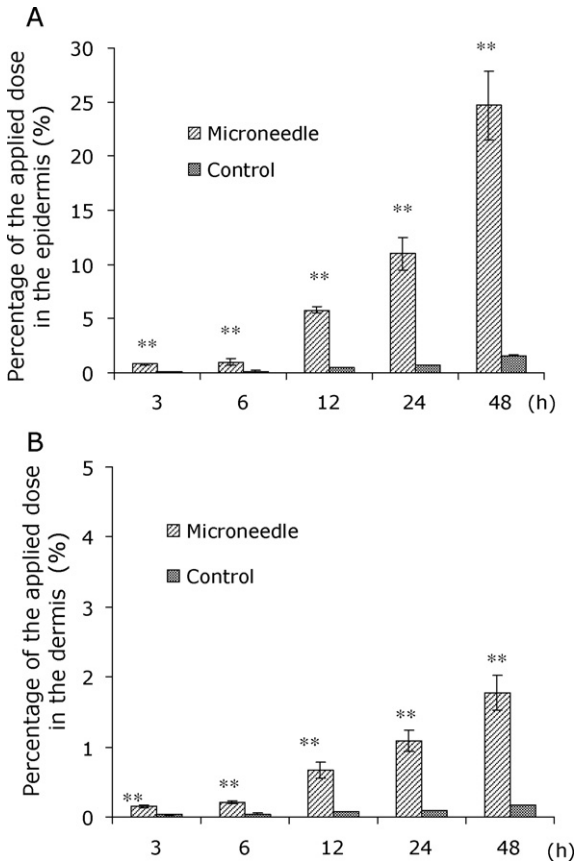

Fig. 4. The percentage of the applied dose of nanoparticles (NP2) depositing in the epidermis (A) and in the dermis (B) within a 48-h period. The skin without microneedles treatment was used in the control groups. Microneedle groups were compared with the control groups. ($n = 6$), $^{**}P < 0.01$.

Fig. 4A and B also shows that with the lapse of time, the percentage of the applied nanoparticles depositing in the epidermis and in the dermis in the microneedle groups increased more rapidly than that in the control groups, implying that the advantage of using microneedles to enhance the intradermal delivery of nanoparticles would be more significant as time passed.

In addition, Fig. 4A and B shows that the percentage of the applied nanoparticles depositing in the epidermis was significantly greater than that in the dermis ($P < 0.01$). This may be due to that the microconduits in the epidermis could serve as reservoirs for nanoparticles to keep retention and progressively diffuse in this skin layer. As no microconduit was created in the dermis, only few nanoparticles could diffuse into this skin layer.

3.7. Effect of nanoparticle size and concentration on penetration

As shown in Fig. 5, the percentage of small nanoparticles penetrated into the skin (epidermis and dermis) was significantly

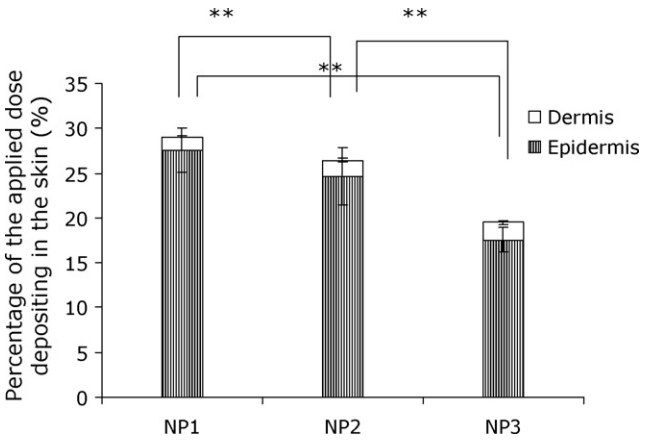

Fig. 5. The percentage of the applied nanoparticles of various sizes depositing in the human skin in the microneedle groups after a 48-h period application. Multiple comparisons among the groups were statistically analyzed. ($n = 6$), $^{**}P < 0.01$.

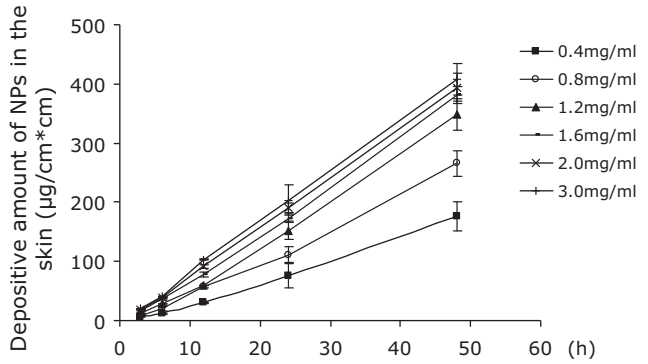

Fig. 6. The amount of nanoparticles of various concentrations depositing in the full-thickness human skin in the microneedle groups after a 48-h period application. ($n = 3$).

greater than that of big nanoparticles ($P < 0.01$), suggesting that the penetration through microconduits was in a size-dependent manner. So reducing the particle size would be beneficial to the penetration. Generally, the amount of the drug loaded in the nanoparticles increases with the nanoparticle size increasing, while the amount of nanoparticles permeated into the skin decreases with the nanoparticle size increasing. To achieve the maximal drug penetration, both of the drug loading efficiency and the nanoparticle size should be considered when nanoparticles are applied for topical drug administration.

Even though the amount of big nanoparticles depositing in the whole skin was lower than that of small nanoparticles, the ratio of the amount of nanoparticles in the dermis to the epidermis increased with the nanoparticle size increasing (Fig. 5). The reason may be that larger particle size could result in that more feeding drug was encapsulated in each nanoparticle, although the amount of big nanoparticles permeating into the dermis may be smaller.

As we know, the nanoparticles size detected by the particle size analyzer is a mean value and the polydispersity index shows the particle size distribution. Since the particle size could influence the penetration of the nanoparticles, the polydispersity index would also affect the penetration. Therefore, reducing the polydispersity index would decrease the variance of the penetration.

Fig. 6 shows that the permeation rate increased with the nanoparticle concentration increasing, but the increase extent decreased gradually. The reason may be that the skin was saturated and the permeation reached a limit value when the concentration gradually increased, so an appropriate concentration with the maximal penetration and the minimum drug-cost should be considered when nanoparticles are used for topical drug administration.

4. Conclusion

CLSM images in our study clearly showed that the nanoparticles were delivered into the skin (epidermis and dermis). Quantitative results indicated that all nanoparticles deposited in the skin; the amount of the nanoparticles depositing in the skin was significantly enhanced by the microneedles; much more nanoparticles located in the epidermis than that in the dermis; the permeation was in a size-dependent manner; the permeation rate of the nanoparticles reached a limit value with the nanoparticle concentration increasing. These results were needed to be further confirmed by an *in vivo* experiment. On basis of *in vitro* experiment results, the biodegradable PLGA nanoparticles would sustain drug release in the skin over a prolonged period. This delivery strategy would prove to be potentially effective for topical drug administration and be used for clinical treatment for dermatological diseases.

Acknowledgments

This work was financially supported by National Science Foundation of China (No. 81000689) and Natural Science Foundation of Shanghai (No. 10ZR1437300).

References

Aguzzi, C., Rossi, S., Bagnasco, M., Lanata, L., Sandri, G., Bona, F., Ferrari, F., Bonferoni, M.C., Caramella, C., 2008. Penetration and distribution of thiocolchicoside through human skin: comparison between a commercial foam (Miotens) a drug solution. AAPS PharmSciTech 9, 1185–1190.

Alvarez-Roman, R., Naik, A., Kalia, Y.N., Fessi, H., Guy, R.H., 2004a. Visualization of skin penetration using confocal laser scanning microscopy. Eur. J. Pharm. Biopharm. 58, 301–316.

Alvarez-Roman, R., Naik, A., Kalia, Y.N., Guy, R.H., Fessi, H., 2004b. Enhancement of topical delivery from biodegradable nanoparticles. Pharm. Res. 21, 1818–1825.

Alvarez-Roman, R., Naik, A., Kalia, Y.N., Guy, R.H., Fessi, H., 2004c. Skin penetration and distribution of polymeric nanoparticles. J. Control. Release 99, 53–62.

Birchall, J., Coulman, S., Anstey, A., Gateley, C., Sweetland, H., Gershonowitz, A., Neville, L., Levin, G., 2006. Cutaneous gene expression of plasmid DNA in excised human skin following delivery via microchannels created by radio frequency ablation. Int. J. Pharm. 312, 15–23.

Chabri, F., Bouris, K., Jones, T., Barrow, D., Hann, A., Allender, C., Brain, K., Birchall, J., 2004. Microfabricated silicon microneedles for nonviral cutaneous gene delivery. Br. J. Dermatol. 150, 869–877.

Coulman, S.A., Anstey, A., Gateley, C., Morrissey, A., McLoughlin, P., Allender, C., Birchall, J.C., 2009. Microneedle mediated delivery of nanoparticles into human skin. Int. J. Pharm. 366, 190–200.

D. Blanco, M.J.A., 1997. Development and characterization of protein-loaded poly (lactic/glycolic acid) nanospheres. Eur. J. Pharm. Biopharm. 43, 285–294.

de Jalon, E.G., Blanco-Prieto, M.J., Ygartua, P., Santoyo, S., 2001. PLGA microparticles: possible vehicles for topical drug delivery. Int. J. Pharm. 226, 181–184.

Gao, X., Tao, W., Lu, W., Zhang, Q., Zhang, Y., Jiang, X., Fu, S., 2006. Lectin-conjugated PEG-PLA nanoparticles: preparation and brain delivery after intranasal administration. Biomaterials 27, 3482–3490.

Henry, S., McAllister, D.V., Allen, M.G., Prausnitz, M.R., 1998. Microfabricated microneedles: a novel approach to transdermal drug delivery. J. Pharm. Sci. 87, 922–925.

Jenning, V., Gysler, A., Schafer-Korting, M., Gohla, S.H., 2000. Vitamin A loaded solid lipid nanoparticles for topical use: occlusive properties and drug targeting to the upper skin. Eur. J. Pharm. Biopharm. 49, 211–218.

Kanikkannan, N., 2002. Iontophoresis-based transdermal delivery systems. BioDrugs 16, 339–347.

Lademann, J., Richter, H., Teichmann, A., Otberg, N., Blume-Peytavi, U., Luengo, J., Weiss, B., Schaefer, U.F., Lehr, C.M., Wepf, R., Sterry, W., 2007. Nanoparticles—an efficient carrier for drug delivery into the hair follicles. Eur. J. Pharm. Biopharm. 66, 159–164.

Liang, W., 2005. New dosage forms of transdermal drug delivery. In: Lu, B. (Ed.), New Techniques and New Dosage Forms of Drugs. People's Medical Publishing House, Beijing, pp. 507–594.

Luengo, J., Weiss, B., Schneider, M., Ehlers, A., Stracke, F., Konig, K., Kostka, K.H., Lehr, C.M., Schaefer, U.F., 2006. Influence of nanoencapsulation on human skin transport of flufenamic acid. Skin Pharmacol. Physiol. 19, 190–197.

McAllister, D.V., Wang, P.M., Davis, S.P., Park, J.H., Canatella, P.J., Allen, M.G., Prausnitz, M.R., 2003. Microfabricated needles for transdermal delivery of

macromolecules and nanoparticles: fabrication methods and transport studies. Proc. Natl. Acad. Sci. U.S.A. 100, 13755–13760.
Pang, Z., Lu, W., Gao, H., Hu, K., Chen, J., Zhang, C., Gao, X., Jiang, X., Zhu, C., 2008. Preparation and brain delivery property of biodegradable polymersomes conjugated with OX26. J. Control. Release 128, 120–127.
Panyam, J., Sahoo, S.K., Prabha, S., Bargar, T., Labhasetwar, V., 2003. Fluorescence and electron microscopy probes for cellular and tissue uptake of poly(D,L-lactide-co-glycolide) nanoparticles. Int. J. Pharm. 262, 1–11.
Prausnitz, M.R., 2004. Microneedles for transdermal drug delivery. Adv. Drug Deliv. Rev. 56, 581–587.
Sugrue, S., 1992. Predicting and controlling colloid suspension stability using electrophoretic mobility and particle size measurements. Am. Lab. 24, 64–71.
Toll, R., Jacobi, U., Richter, H., Lademann, J., Schaefer, H., Blume-Peytavi, U., 2004. Penetration profile of microspheres in follicular targeting of terminal hair follicles. J. Invest. Dermatol. 123, 168–176.
Verbaan, F.J., Bal, S.M., van den Berg, D.J., Groenink, W.H., Verpoorten, H., Luttge, R., Bouwstra, J.A., 2007. Assembled microneedle arrays enhance the transport of compounds varying over a large range of molecular weight across human dermatomed skin. J. Control. Release 117, 238–245.
Xie, Y., Xu, B., Gao, Y., 2005. Controlled transdermal delivery of model drug compounds by MEMS microneedle array. Nanomedicine 1, 184–190.